

Effective Stochastic Resonance under Heterogeneous Amplitude of Noise

Shogo Torigoe¹, Ryosuke Kawai¹, Kazuhiro Yoshida², Akinori Awazu¹, and Hiraku Nishimori^{1*}

¹*Department of Mathematical and Life Sciences, Hiroshima University,
Kagamiyama, Higashi-hiroshima 739-8526, Japan and*

²*Department of Mathematical Sciences, Osaka Prefecture University, Sakai 599-8531, Japan*

(Dated: February 22, 2024)

Effective stochastic resonance (SR) is numerically and analytically studied using a model with coupled two particles exposed to heterogeneous, i.e., particles dependent, amplitude of noise. Compared to previous SR models of single particle and to those of coupled two particles exposed to equivalent amplitude of noise, the present model exhibits a more intensive resonance of, at least, one particle exposed to the non-larger amplitude of noise with the assistance of another particle. In a certain range of conditions, this effective resonance of one particle overwhelms the poor resonance of the other particle, meaning that heterogeneous amplitude of noise leads the system, not only locally but also in the average of the whole, to the effective SR.

I. INTRODUCTION

As reviewed in¹, various kinds of phenomena have been recognized as stochastic resonance phenomena (SR) and have been studied with a variety of methods²⁻⁹. Among theoretical models for SR, the simplest is that described by the Langevin dynamics of a particle confined in a double-well potential periodically deformed by an oscillating external field,

$$\frac{\partial x}{\partial t} = -\frac{\partial V(x)}{\partial x} + \xi(t), \quad (1)$$

where,

$$V(x) = -ax^2 + bx^4 - A \cos(\Omega t)x, \quad (2)$$

the last term of which indicates the oscillating external field. Hereafter, we call the above model as the original SR model.

To quantify the efficiency of SR, the signal-to-noise ratio (SNR), the Spectral Power Amplification (SPA) and other quantities have been proposed. According to recent relating studies¹³, here, we employ SPA as the index of SR. SPA is, roughly, the power ratio between the input and the output signals, and is defined as,

$$\frac{\int_{\Omega-\delta}^{\Omega+\delta} S_{out}(\omega) d\omega}{\int_{\Omega-\delta}^{\Omega+\delta} S_{in}(\omega) d\omega}, \quad (3)$$

where Ω , $S_{in}(\omega)$ and $S_{out}(\omega)$ represent the frequency of the input signal, power spectrums of input and output signals, respectively. The denominator means the power of the input signal (sinusoidal wave), and the numerator is the corresponding power of the output signal. Here, δ is taken to be larger than the peak width of the power spectrum. In our simulation, considering the resolution of the numerical Fourier transformation, (3) is approximated by

$$\frac{S_{out}(\Omega)}{S_{in}(\Omega)}. \quad (4)$$

A series of efforts to obtain the higher SPA or SNR have been conducted through variations of the original SR model, one of which was made by coupling two particles applied in a common double-well potential periodically deformed by the external field as described by (2). Through the reasonable tuning of coupling strength, this coupled particles model gives a higher SNR than the original SR model^{11,12}. As another directional variation, cascade dynamics using one-way coupling between oscillating sub-systems was simulated¹⁰, that exhibits a high synchronization to the oscillating external field by adding a proper amplitude of noise even below Hopf bifurcation threshold. Note that most of the previous models of SR have treated systems in which constituent elements are exposed to equivalent amplitude of noise, whereas a few models have considered the heterogeneous, i.e., element dependent, amplitudes of noise. As discussed in one of such models⁸, the noise emerging in a living cell is not always equivalent through the cell because the origin of noise in living systems is, in addition to the thermal fluctuation, the local density fluctuation of reacting molecules in each cell.

Therefore, as one way for revising the preceding SR models considering at the time the potential comparison to actual systems, we study SR model of coupled two elements exposed to the heterogeneous amplitude of noise, restricting the model as simple as possible to focus only on the basic mechanism of the underlying system.

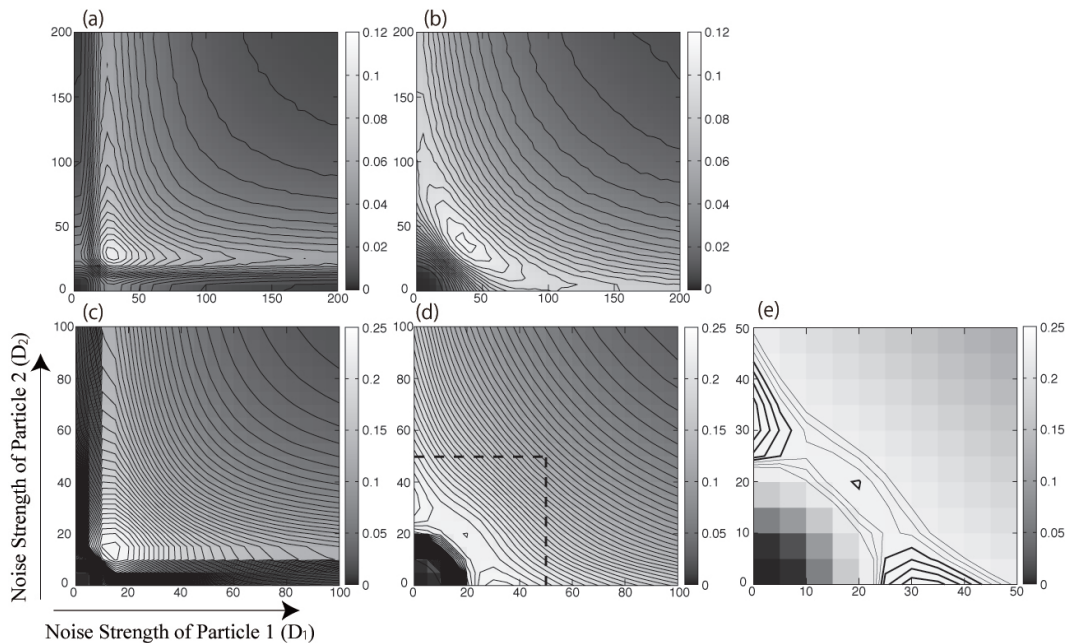


FIG. 1: Contour lines of ASPA in $D_1 - D_2$ space for (a) $K = 1.00, \Omega = \pi/4$, (b) $K = 5.00, \Omega = \pi/4$, (c) $K = 1.00, \Omega = \pi/64$, (d) $K = 5.00, \Omega = \pi/64$, (e) extended figure of the left-lower part of (d). The brighter tone means the higher value of ASPA. ASPA is symmetric with respect to the diagonal line $D_1 = D_2$ from the definition of ASPA. Only in the case of (d) (and (e)), the peaks of ASPA fall off the diagonal, equivalent amplitude of noise, line. In (d), contours of $\text{ASPA} \geq 0.230$ are drawn by bolder lines and those of $\text{ASPA} < 0.222$ are abbreviated to focus on the maximum points

II. LANGEVIN DYNAMICS MODEL AND SIMULATIONS

The present model is described as,

$$\begin{aligned} \frac{\partial x_1}{\partial t} &= -\frac{\partial V(x_1)}{\partial x_1} + K(x_2 - x_1) + \xi_1(t), \\ \frac{\partial x_2}{\partial t} &= -\frac{\partial V(x_2)}{\partial x_2} + K(x_1 - x_2) + \xi_2(t), \end{aligned} \quad (5)$$

where $V(x)$ is same as (2), $a = 8.0$, $b = 0.25$, $A = 10.0$ and K is coupling constant. The quantities $\xi_1(t)$ and $\xi_2(t)$ are Gaussian white noise with the relations,

$$\langle \xi_i(t) \rangle = 0, \quad \langle \xi_i(t) \xi_j(s) \rangle = 2D_i \delta_{i,j} \delta(t-s) \quad (i, j \in \{1, 2\}). \quad (6)$$

It should be notified that noise amplitudes D_1 and D_2 are *independently* varied as a set of control parameters. We numerically calculate (5) and measure SPA for respective particles with varying a set of parameters (D_1, D_2, K). The numerical integration is carried out using the 4th order Runge-Kutta method for deterministic part and the Euler-Maruyama scheme for stochastic part with time mesh $\Delta t = 0.005$. All data are taken as the ensemble averages of 100 simulations with each run performed from $t = 0$ to $t = 102 \times 2\pi/\Omega$ under the randomly chosen initial conditions of x_i ($x_i \in \{-\sqrt{a/2b}, \sqrt{a/2b}\}$), where we take away the dynamics from $t = 0$ to $t = 2 \times 2\pi/\Omega$ to avoid the dependence to initial conditions. In the following, we show the numerical outcomes. Specifically, SPA of particle 1 named SPA1, and the average SPA of two particles named $\text{ASPA} = (\text{SPA1} + \text{SPA2})/2$, are focused on.

Fig.1 shows ASPA in $D_1 - D_2$ parameter space for different sets of (K, Ω). Note that Fig.1(a)-(d) are symmetric with respect to the diagonal line $D_1 = D_2$ from the above definition of ASPA. As the oscillation frequency of external field, two values, $\Omega = \pi/4$ and $\Omega = \pi/64$, are chosen, and as the coupling strength, $K = 1.00$ and $K = 5.00$ are chosen. Fig.1(a) and (b) show ASPA numerically obtained with $\Omega = \pi/4$ in the cases of weak ($K = 1.00$) and strong ($K = 5.00$) couplings, respectively. For both cases, the peaks of ASPA roughly falls on the line $D_1 = D_2 > 0$ meaning that equivalent amplitude of noise leads the system to the most effective SR in $D_1 - D_2$ space in these cases of $\Omega = \pi/4$. With a slower oscillation ($\Omega = \pi/64$) of external field, if coupling strength is weaker than a critical value, the equivalent amplitude of noise still gives the largest ASPA as seen in Fig.1(c). On the other hand, as shown in

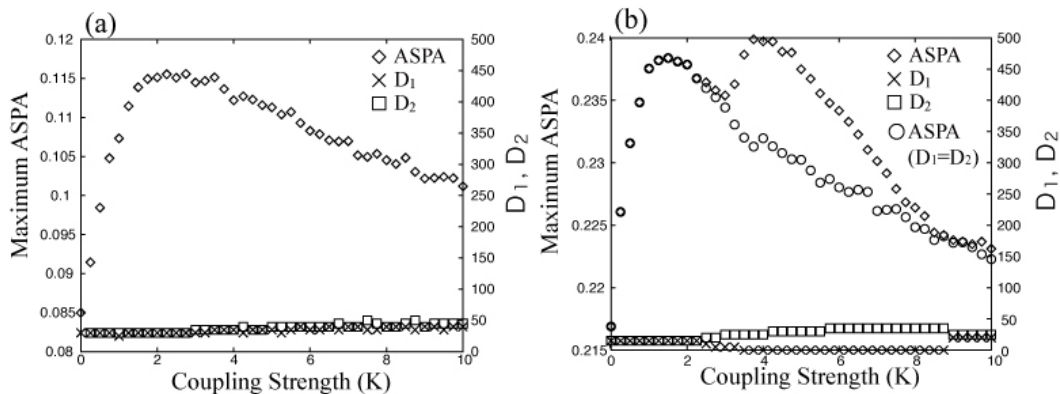


FIG. 2: Maximum ASPA obtained in each $D_1 - D_2$ space with different K value (\diamond), Maximum ASPA obtained under equivalent noise ($D_1 = D_2$) (\circ), and corresponding set (D_1, D_2) (\square and \times) for (a) $\Omega = \pi/4$, (b) $\Omega = \pi/64$, here, only the sets satisfying $D_1 \leq D_2$ are drawn.

Fig.1(d) (and its enlarged view Fig.1(e)) for a stronger coupling ($K = 5.00$) with $\Omega = \pi/64$, the peaks of ASPA in $D_1 - D_2$ space are definitely located *off* the equivalent amplitude line of noise. This means that heterogeneous amplitude of noise leads the system to the most effective SR in $D_1 - D_2$ space in this case.

In Fig.2, maximum ASPAs obtained at each K -fixed $D_1 - D_2$ space (hereafter max-ASPA) are connected, varying K , as graphs. The symbol \diamond in Fig.2(a) shows the relation between K and max-ASPA in the case of $\Omega = \pi/4$. Here, SR of the system is reinforced as the coupling between particles is strengthened until max-ASPA reaches a peak value at finite K ($K \simeq 2$). In the same figure, the symbols, \square and \times respectively give the sets (D_1, D_2) realizing max-ASPA at each K . As mentioned above, the value of ASPA is symmetric with respect to D_1 and D_2 from the definition of ASPA, therefore two sets of (D_1, D_2) realizing max-ASPA are seen if $D_1 \neq D_2$. Fig.2 (and Fig.4) show only the sets satisfying $D_1 \geq D_2$. Two symbols \square and \times roughly collapse on each other in Fig.2(a) indicating that max-ASPA is attained under equivalent amplitude of noise in this case. Fig.2(b) shows the case of slower oscillation $\Omega = \pi/64$. Like in Fig.2(a), the symbol \diamond shows the relation between K and max-ASPA in each K -fixed $D_1 - D_2$ space. In this figure, max-ASPA graph consists of two parts divided by a dip around $K \simeq 3$, each of which has a mound shape, and as mentioned afterward, the right-side mound including the highest point in the graph is mainly contributed by the particle exposed to the lower amplitude of noise. The symbols, \square and \times , in the same figure give the set (D_1, D_2) of noise amplitude with which max-ASPA is realized at each K . Obviously different from the case of $\Omega = \pi/4$ shown in Fig.2(a), D_1 and D_2 in Fig.2(b) separate from each other for $2.25 \leq K \leq 9.25$, within which interval the highest value of the max-ASPA is realized. Namely, the most effective SR in $D_1 - D_2$ space is realized when heterogeneous amplitude of noise is applied to the system. To close up further the effect of heterogeneous amplitude of noise, we plot in Fig.2(b) maximum ASPA obtained along $D_1 = D_2$ line in each K -fixed $D_1 - D_2$ space. Compared with max-ASPA obtained without the constraint $D_1 = D_2$ in the same figure, we see the right-side mound in max-ASPA graph is definitely ascribed to the heterogeneity of adding noise.

In the next, we concentrate on the SR of particle 1. Fig.3(a)-(d) show SPA1 (SPA of particle 1) in $D_1 - D_2$ space for different sets of (K, Ω). The peaks in all of these figures are located *off* the diagonal line $D_1 = D_2$ and within the area of $D_1 < D_2$. This means that the particle under a smaller amplitude of noise dominantly experiences the effective SR caused by the heterogeneous amplitude of noise (hereafter, heterogeneous SR). Fig.4(a) and (b) show the relation between K and maximum SPA of particle 1 (hereafter max-SPA1) in the cases of $\Omega = \pi/4$ and $\Omega = \pi/64$ respectively, where the sets (D_1, D_2) realizing max-SPA1 in each K fixed $D_1 - D_2$ space also are drawn. In the same figures, for the easiness of comparison, fitting curves of the max-ASPA shown in Fig.2(a) and (b) are added as dashed lines, where the graphs of max-SPA1 start from the values same as max-ASPA at $K = 0$. In the small K region, as K increases, the values of max-SPA1 monotonically increase, and after passing over shoulder parts around which the increasing rates once decreases, they recover rapid increasing rate until reaching maximum values. Through whole range of K , max-SPA1 is kept higher than (or at least same as) the max-ASPA of dashed lines. This, again, means that the particles under a smaller amplitude of noise dominantly experiences the effect of the heterogeneous SR.

If we pay attention to the K value ($K \geq 5.75$) realizing the peak of max-SPA1 in Fig.4(a) and the decreasing curve of max-ASPA around the corresponding K value, the SR of particle 1 is considered not sufficiently significant to be reflected in the average SR of the whole system in this case of $\Omega = \pi/4$. Meanwhile, as shown in Fig.4(b), with the slower oscillation of $\Omega = \pi/64$, the K value giving the peak of max-SPA1 realizes the peak of max-ASPA at the same time. Namely, the resonance effect of particle 1 is strong enough to overcome the poor resonance of particle 2 in this case of slow oscillation ($\Omega = \pi/64$) of external field. In such way, heterogeneous amplitude of noise leads the system

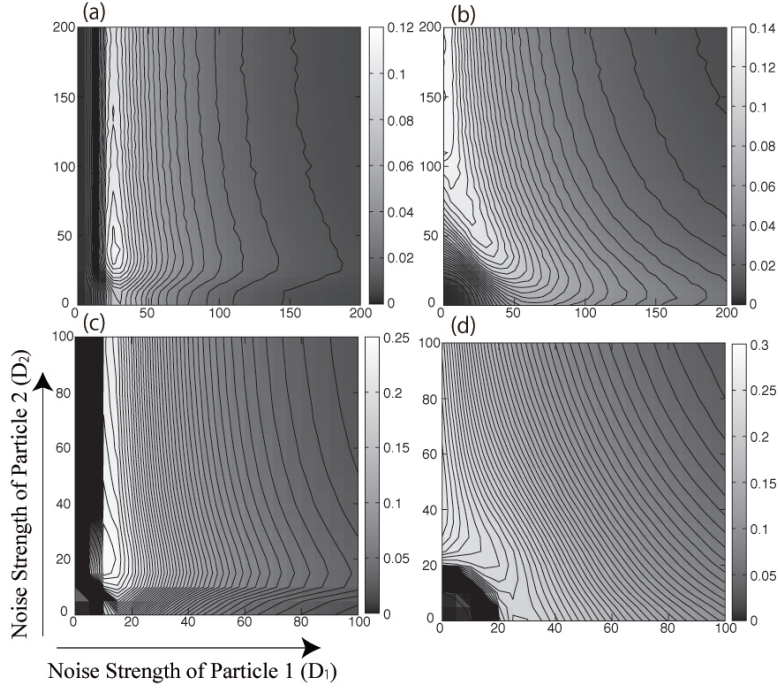


FIG. 3: Contour lines of SPA1 in $D_1 - D_2$ space for (a) $K = 1.00$, $\Omega = \pi/4$, (b) $K = 5.00$, $\Omega = \pi/4$, (c) $K = 1.00$, $\Omega = \pi/64$, (d) $K = 5.00$, $\Omega = \pi/64$. The brighter tone means the higher value of SPA1.

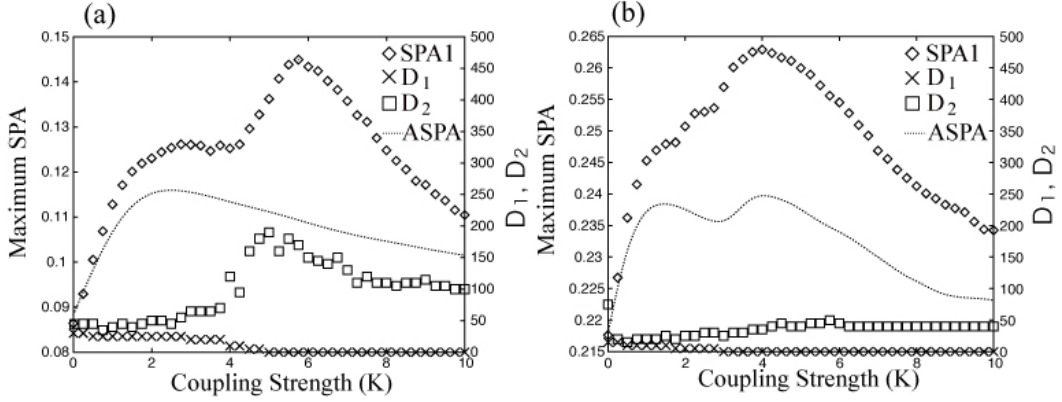


FIG. 4: Maximum SPA1 obtained in each K -fixed $D_1 - D_2$ space (\diamond), fitting curve of Maximum ASPA (dashed line), and corresponding sets (D_1, D_2) (\square and \times) for (a) $\Omega = \pi/4$, (b) $\Omega = \pi/64$. Here, only the sets satisfying $D_1 \leq D_2$ are drawn.

in a certain range of conditions, not only locally but also in the average of the whole, to an effective SR.

III. ANALYSIS USING MASTER EQUATION MODEL

To understand the mechanism of the present effective SR of coupled two particles under heterogeneous amplitude of noise, we analytically treat the simplified transient dynamics among finite number of states using a master equation;

$$\begin{aligned} & \frac{dP(\sigma_1, \sigma_2, t)}{dt} \\ &= W(-\sigma_1, \sigma_2, t)P(-\sigma_1, \sigma_2, t) - W(\sigma_1, \sigma_2, t)P(\sigma_1, \sigma_2, t) + W(-\sigma_2, \sigma_1, t)P(\sigma_1, -\sigma_2, t) - W(\sigma_2, \sigma_1, t)P(\sigma_1, \sigma_2, t), \end{aligned} \quad (7)$$

where $\sigma_i \in \{s, -s\}$ represents the state in which particle $i \in \{1, 2\}$ is at the left minima ($\sigma_i = -s$) or the right minima ($\sigma_i = s$) of the potential expressed by (2) ($s = \sqrt{a/2b}$). $W(\sigma_i, \sigma_j, t)$ denotes the transition rate from state (σ_i, σ_j) to

$(-\sigma_i, \sigma_j)$, the specific form of which is assumed as,

$$W(\sigma_i, \sigma_j, t) = \frac{1}{2\tau_i} \{1 - \sigma_i \sigma_j \tanh(K/D_i)\} \{1 - \sigma_i \tanh(A \cos \Omega t/D_i)\} \quad (i \neq j), \quad (8)$$

where A , K , D_i are the amplitude of the input signal, the coupling strength and the noise strength added to the particle i , respectively. The quantity τ_i is the Arrhenius-type relaxation time, $\tau_i = \tau_0 \exp(\Delta/D_i)$, where $\tau_0 = 2\pi/\sqrt{(|-2a+k|(4a+k))}$ and Δ is the activation energy. This transition rate has a similar form as that introduced in the kinetic Ising model for $D_1 = D_2$ ⁹. Here, we should note that this master equation model does not take into account the direct transition between states (σ_1, σ_2) and $(-\sigma_1, -\sigma_2)$. It indicates that this model has a direct correspondence to (5) only at the weak coupling between two particles.

As shown in Appendix, master equation (7) is analytically solved with several approximations introduced in ref(9) for $D_1 = D_2$ though some details of calculation are different for the present case of $D_1 \neq D_2$. Fig.5(a)-(d) show ASPA obtained using the analytical solution of (7) in $D_1 - D_2$ space with different sets of (K, Ω) .

In Fig.5(a) and (b), the peak of ASPA falls on the line $D_1 = D_2 > 0$ which means the equivalent noise leads the system to the most effective SR in $D_1 - D_2$ space. This figures qualitatively corresponds to Fig.1(a) and (b). With slower oscillation $\Omega = \pi/64$ and weak coupling $K = 1.00$ the peak of ASPA is still on the diagonal line $D_1 = D_2 > 0$ as shown in Fig.5(c), however the peaks of ASPA fall *off* the diagonal line with stronger coupling $K = 5.00$ (Fig.5(d)) meaning that heterogeneous amplitude of noise drives the system to the most effective SR in $D_1 - D_2$ space. In this way, as long as looking the contours of ASPA, qualitative features of Fig.1(a)-(d) obtained by the simulation of Langevin dynamics model (5) seems to be reproduced by the analytical solution of master equation (7). However some remarkable aspects of the heterogeneous SR are not sufficiently described by the present form of master equation model as discussed in the followings.

To discuss the quantitative aspects, max-ASPAs obtained at each K -fixed $D_1 - D_2$ space are connected in Fig.6 as graphs with varying K . Solid lines in Fig.6(a), (b) show the relation between K and max-ASPAs in the cases of $\Omega = \pi/4$ and $\Omega = \pi/64$, respectively. Here, SR of the system is reinforced as the coupling between particles is strengthened until max-ASPAs reach peak values at finite K ($K \simeq 0.6$ in Fig.6(a) and $K \simeq 0.7$ in Fig.6(b)), and thereafter monotonically decrease. In the same figures, dashed and broken lines respectively give D_1 and D_2 which

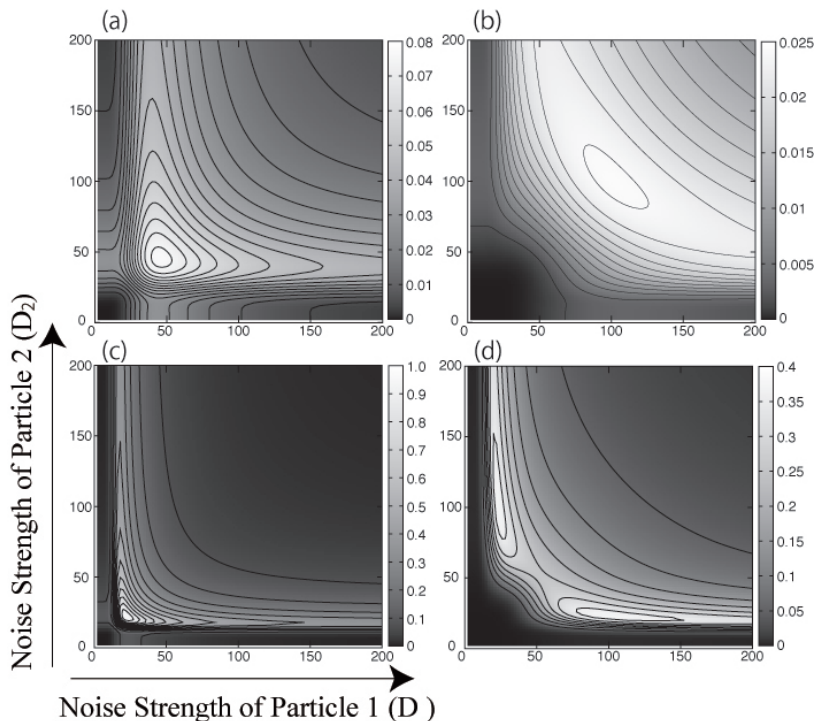


FIG. 5: Contour lines of ASPA in $D_1 - D_2$ space for (a) $K = 1.00$, $\Omega = \pi/4$, (b) $K = 5.00$, $\Omega = \pi/4$, (c) $K = 1.00$, $\Omega = \pi/64$, (d) $K = 5.00$, $\Omega = \pi/64$, $A = 10.0$, $\tau_0 = 2\pi/\sqrt{(|-2a+k|(4a+k))}$, $\Delta = 64.0$ obtained from the analytical calculation of master equation (7). The brighter tone means the higher value of ASPA. ASPA is symmetric with respect to D_1 and D_2 from the definition of ASPA. In the case of (d), the ASPA has two peaks and the peaks fall *off* the diagonal line.

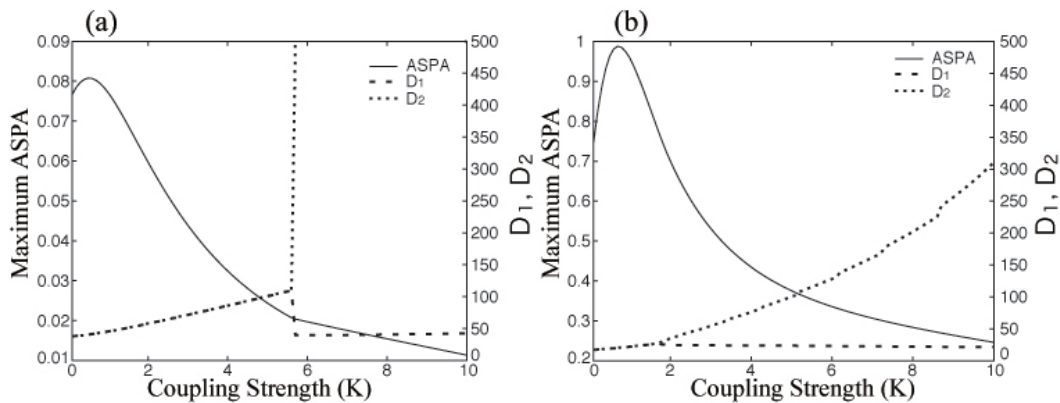


FIG. 6: Maximum ASPA obtained in each K -fixed $D_1 - D_2$ space (solid line), and corresponding sets (D_1, D_2) (D_1 : dashed line, D_2 : broken line) for (a) $\Omega = \pi/4$, (b) $\Omega = \pi/64$. Here, only the sets satisfying $D_1 \leq D_2$ are drawn and $A = 10.0$, $\tau_0 = 2\pi/\sqrt{|-2a+k|(4a+k)}$, $\Delta = 64.0$. The curve of D_2 in (a) comes out of the graph over a critical value of K .

collapse on each other in a range of small K and separate beyond Ω -dependent critical values of K . The effect of the heterogeneous amplitude of noise exceeds that of equivalent noise as K increases. These features shown in Fig.6 especially for $K < 3$ reflect the qualitative characters obtained by Langevin dynamics model (Fig.2) for the same K range. However, it should be cared in Fig.6(b), that the effect of heterogeneous amplitude of noise is not sharp enough to make the second mound of the max-ASPAs graph shown in Fig.2(b) of Langevin dynamics model, nor the overlap of D_1 and D_2 in Fig.2(b) giving max-ASPAs for large K is recognized in Fig.6(b). Moreover the dominant region of heterogeneous SR for large K in Fig.6(a) has no counterpart in Fig.2(a).

IV. DISCUSSION AND SUMMARY

These distinctions between behaviors of the Langevin dynamics model and the master equation model would partially originate from the assumption of weak coupling limit as mentioned in the previous section. However the more intrinsic origin for this distinction seems linked to the basic mechanism of the present heterogeneous SR as explained below;

If we rewrite the Langevin dynamics of (5) like,

$$\begin{aligned} \frac{\partial x_1}{\partial t} &= -\frac{\partial V_{\text{eff}}(x_1, x_2)}{\partial x_1} + \xi_1(t), \\ \frac{\partial x_2}{\partial t} &= -\frac{\partial V_{\text{eff}}(x_1, x_2)}{\partial x_2} + \xi_2(t), \end{aligned} \quad (9)$$

an overall effective potential $V_{\text{eff}}(x_1, x_2)$ for particles 1 and 2 is,

$$V_{\text{eff}}(x_1, x_2) = a(x_1^2 + x_2^2) + b(x_1^4 + x_2^4) + K(x_1 - x_2)^2 - A \cos(\Omega t)(x_1 + x_2). \quad (10)$$

If we take x_2 as constant in the above form, an effective potential of particle 1 becomes monostable above a critical coupling strength K_c that depends on Ωt and x_2 . Then the signal and the coupling force act in the same direction if $\Omega t = 0$, $x_2 = s (= \sqrt{a/2b})$, (or if $\Omega t = \pi$ and $x_2 = -s (= -\sqrt{a/2b})$), supposing coupling strength satisfies $K > K_c$, in which case the signal is superthreshold. This means that particle 1 will move quickly into the single minimum (if it is not already there) without surmounting a potential barrier. Noise is not necessary for this transition of particle 1. On the other hand, particle 2 should be sufficiently noisy to trigger the monostable potential for particle 1. In particular, the mean escape time of particle 2 should be much smaller than half the period of the signal. In this case, particle 1 can exhibit essentially a classical (i.e., deterministic) resonance, which results in a large ASPA at unequal noise amplitudes. In the present simulation of Langevin dynamics model, the critical coupling strength K_c is estimated as $K_c \simeq 2.4$ using the specific values of parameters: $a = 8.0, b = 0.25, A = 10.0$.

This scenario explains the split of max-ASPAs graphs over $K \simeq 2.4 \simeq K_c$ in Fig.2(b), one is max-ASPAs within whole $D_1 - D_2$ space and the other is that on $D_1 = D_2$ line. Also K_c is close to the initiating point of the right-side mound of max-ASPAs in the same figure. Moreover, it should be noted that, in the limit $K \rightarrow \infty$, max-ASPAs in

$D_1 - D_2$ space degenerates on a line $D_1 + D_2 = \text{constant}$, causing the vanishment of heterogeneous SR in this limit, which is reflected in Fig.2(b) as the rejoining of D_1 and D_2 at large K accompanied with the rejoining of max-ASPA values in whole $D_1 - D_2$ space and along $D_1 = D_2$ line in the same figure.

To summarize, we numerically showed that the efficiency of SR is enhanced by the coupling of bistable elements exposed to heterogeneous amplitude of noise. This heterogeneous SR is caused through a 'task allocation' between two particles such that one particle (particle 2) under large fluctuation easily jumps over the potential barrier and pulls another particle (particle 1) to the potential minimum state keeping itself under a large fluctuation, then only the latter (particle 1) directly contributes to the heterogeneous SR. Therefore if we focus only on the SR of particle 1, it is found that the present mechanism works for a wide range in K (coupling strength) and Ω (frequency of external signal) as seen in Fig.4, where the maximum value of SPA1, an SR index of particle 1, is marked under heterogeneous amplitude of noise in almost all range of K in the graph.

However, the most noticeable in the present study is that the effect of heterogeneous SR is largely pronounced when coupling strength between two particles exceeds a critical value and the external signal for particle 1 reaches super-threshold level with the help of highly fluctuating particle 2. In that case not only SPA1; an index of SR of particle 1, but also ASPA; an index of averages degree of SR of particles 1 and 2, mark the maximum value at each- K under heterogeneous amplitude of noise.

In this way, the present heterogeneous SR is an outcome of an exquisite combination of the triggering particle with a large fluctuation and the following particle which faithfully responds to the external signal under small (or zero) amplitude of noise. We suppose that the heterogeneous SR has potential applicability to a wider variety of stochastic resonance phenomena like those of devising artificial sensors with high susceptibility¹⁴, and that it has a certain connection to the basic study on the function of non-isothermal multi-elements systems¹⁴.

Acknowledgments

This study was supported by Grant-in-Aid (19654056, 22540391) for Scientific Research, and, the Global COE Program G14 (Formation and Development of Mathematical Sciences Based on Modeling and Analysis) of JSPS.

Appendix

In this appendix, we analytically derive the time evolution of the expectation values of σ_i treated in (7). For simplification we assume $\sigma_i \in \{1, -1\}$. From equation (7), we obtain the dynamics for the expectation values,

$$\tau_1 \langle \dot{\sigma}_1 \rangle = -\langle \sigma_1 \rangle + \tanh(\beta_1 A \cos(\Omega t)) + \eta_1 \langle \sigma_2 \rangle - \eta_1 \tanh(\beta_1 A \cos(\Omega t)) \langle \sigma_1 \sigma_2 \rangle, \quad (\text{A.1})$$

$$\tau_2 \langle \dot{\sigma}_2 \rangle = -\langle \sigma_2 \rangle + \tanh(\beta_2 A \cos(\Omega t)) + \eta_2 \langle \sigma_1 \rangle - \eta_2 \tanh(\beta_2 A \cos(\Omega t)) \langle \sigma_1 \sigma_2 \rangle, \quad (\text{A.2})$$

$$\begin{aligned} \langle \sigma_1 \sigma_2 \rangle &= \frac{1}{\tau_1} (-\langle \sigma_1 \sigma_2 \rangle + \eta_1 + \tanh(\beta_1 A \cos(\Omega t)) \langle \sigma_2 \rangle - \eta_1 \tanh(\beta_1 A \cos(\Omega t)) \langle \sigma_1 \rangle) \\ &\quad + \frac{1}{\tau_2} (-\langle \sigma_1 \sigma_2 \rangle + \eta_2 + \tanh(\beta_2 A \cos(\Omega t)) \langle \sigma_1 \rangle - \eta_2 \tanh(\beta_2 A \cos(\Omega t)) \langle \sigma_2 \rangle), \end{aligned} \quad (\text{A.3})$$

where $\eta_i \equiv \tanh(K\beta_i)$ and $\beta_i \equiv 1/D_i$. To solve the equation, we assume that input signal is sufficiently weak ($\beta_i A \ll 1$), then, the correlation function $\langle \sigma_1(t) \sigma_2(t) \rangle$ has even parity with respect to A . Consequently, only the zeroth order term in A remains in this correlation in the linear approximation. An additional assumption is that $\langle \sigma_1(t) \sigma_2(t) \rangle$ is in a steady state, which means that $\langle \sigma_1(t) \sigma_2(t) \rangle$ is expressed like,

$$\langle \sigma_1 \sigma_2 \rangle = \frac{\eta_1 \tau_2 + \eta_2 \tau_1}{\tau_1 + \tau_2}. \quad (\text{A.4})$$

Then (A1) and (A2) are simplified like,

$$\begin{aligned} \begin{bmatrix} \langle \dot{\sigma}_1 \rangle \\ \langle \dot{\sigma}_2 \rangle \end{bmatrix} &= \begin{bmatrix} -\frac{1}{\tau_1} & \frac{\eta_1}{\tau_1} \\ \frac{\eta_2}{\tau_2} & -\frac{1}{\tau_2} \end{bmatrix} \begin{bmatrix} \langle \sigma_1 \rangle \\ \langle \sigma_2 \rangle \end{bmatrix} + \begin{bmatrix} H_1 \cos(\Omega t) \\ H_2 \cos(\Omega t) \end{bmatrix}, \\ H_1 &= \frac{(1 - \eta_1 \langle \sigma_1 \sigma_2 \rangle) \beta_1 A}{\tau_1}, \\ H_2 &= \frac{(1 - \eta_2 \langle \sigma_1 \sigma_2 \rangle) \beta_2 A}{\tau_2}. \end{aligned} \quad (\text{A.5})$$

The long time limit solution of the above equation is

$$\langle \sigma_i(t) \rangle_{\text{longtime}} = R_{i1} \cos(\Omega t - \varphi_1) - R_{i2} \cos(\Omega t - \varphi_2) = R_i \cos(\Omega t - \psi_i) \quad (i \in \{1, 2\}), \quad (\text{A.6})$$

where,

$$\begin{aligned} \lambda_1 &= \frac{1}{2} \left(-(\rho_1 + \rho_2) + \sqrt{(\rho_1 - \rho_2)^2 + 4\eta_1\eta_2\rho_1\rho_2} \right), \\ \lambda_2 &= \frac{1}{2} \left(-(\rho_1 + \rho_2) - \sqrt{(\rho_1 - \rho_2)^2 + 4\eta_1\eta_2\rho_1\rho_2} \right), \\ L &= 2\eta_1\rho_1, \\ M &= (\rho_1 - \rho_2) + \sqrt{(\rho_1 - \rho_2)^2 + 4\eta_1\eta_2\rho_1\rho_2}, \\ N &= (\rho_1 - \rho_2) - \sqrt{(\rho_1 - \rho_2)^2 + 4\eta_1\eta_2\rho_1\rho_2}, \\ R_{11} &= \frac{NH_1 - LH_2}{(N - M)\sqrt{\lambda_1^2 + \Omega^2}}, \\ R_{12} &= \frac{-MH_1 + LH_2}{(N - M)\sqrt{\lambda_2^2 + \Omega^2}}, \\ R_{21} &= \frac{M(NH_1 - LH_2)}{L(N - M)\sqrt{\lambda_1^2 + \Omega^2}}, \\ R_{22} &= \frac{N(-MH_1 + LH_2)}{L(N - M)\sqrt{\lambda_2^2 + \Omega^2}}, \\ R_i &= \sqrt{R_{i1}^2 + R_{i2}^2 + 2R_{i1}R_{i2} \cos(\varphi_1 - \varphi_2)}, \\ \varphi_i &= \tan^{-1} \left(\frac{\Omega}{\lambda_i} \right), \\ \psi_i &= \tan^{-1} \left(\frac{R_{i1} \sin \varphi_1 + R_{i2} \sin \varphi_2}{R_{i1} \cos \varphi_1 + R_{i2} \cos \varphi_2} \right), \\ \rho_i &\equiv \frac{1}{\tau_i}, \\ \Gamma_i &\equiv \exp(\lambda_i t - \lambda_i t_0). \end{aligned}$$

Hence, the auto-correlation function is

$$\langle \sigma_i(t + \Delta t) \sigma_i(t) \rangle_{\text{longtime}} = R_i^2 \cos(\Omega t + \Omega \Delta t - \psi_i) \cos(\Omega t - \psi_i), \quad (\text{A.7})$$

and averaging it over initial phase, we get

$$\begin{aligned} \langle \langle \sigma_i(t + \Delta t) \sigma_i(t) \rangle \rangle &= \frac{\Omega}{2\pi} \int_0^{2\pi/\Omega} \langle \sigma_i(t + \Delta t) \sigma_i(t) \rangle_{\text{longtime}} dt \\ &= \frac{R_i^2 \cos(\Omega \Delta t)}{2}. \end{aligned} \quad (\text{A.8})$$

To obtain the power spectra, we apply the Wiener-Khinchin theorem to (A.8). The power spectrum $S_i(\omega)$ defined by

$$S_i(\omega) = \int_{-\infty}^{\infty} e^{-i\omega \Delta t} \langle \langle \sigma_i(t + \Delta t) \sigma_i(t) \rangle \rangle d\Delta t, \quad (\text{A.9})$$

is calculated in the form

$$S_i(\omega) = \frac{\pi R_i^2}{2} \left[\delta(\Omega - \omega) + \delta(\Omega + \omega) \right]. \quad (\text{A.10})$$

And the power spectrum about input signal ($A \cos(\Omega t)$) is written as

$$\begin{aligned} S_{in}(\omega) &= \int_{-\infty}^{\infty} \langle A \cos(\Omega t + \Omega \Delta t) A \cos(\Omega t) \rangle \exp(-i\omega \Delta t) d\Delta t \\ &= \frac{\pi A^2}{2} (\delta(\Omega - \omega) + \delta(\Omega + \omega)). \end{aligned} \quad (\text{A.11})$$

By substituting S_i for S_{out} in (4), we obtain the local SPA, i.e. SPA_i ($i \in \{1, 2\}$), and the average SPA, i.e. ASPA,

$$SPA_i = \frac{R_i^2}{A^2}, \quad (\text{A.12})$$

$$ASPA = \frac{SPA_1 + SPA_2}{2} = \frac{R_1^2 + R_2^2}{2A^2}. \quad (\text{A.13})$$

In the present case of $\sigma \in \{s, -s\}$, to comparing with Langevin Equation (5) $R_i(K, A)$ is written as $R_i(s^2 K, sA)$, the expectation value σ_i and SPA also are simply rewritten as

$$\langle \sigma_i \rangle_{\text{longtime}} = s R_i(s^2 K, sA) \cos(\Omega t - \psi_i), \quad (\text{A.14})$$

$$SPA_i = \frac{s^2 R_i(s^2 K, sA)^2}{A^2}. \quad (\text{A.15})$$

- * Electronic address: nishimor@hiroshima-u.ac.jp
- ¹ L. Gammaitoni, P. Hänggi, P. Jung, F. Marchesoni, *Reviews of Modern Physics*, **70** (1998) 223.
 - ² R. Benzi, A. Sutera, A. Vulpiani, *J. Phys. A*, **14** (1981) L453.
 - ³ J.K. Douglass, L. Wilkens, E. Pantazelou, F. Moss, *Nature*, **365** (1993) 337.
 - ⁴ J.P. Levin, J.P. Miller, *Nature*, **380** (1996) 165.
 - ⁵ J.J. Collins, T.T. Imhoff, P. Grigg, *Journal of Neurophysiology*, **76** (1996) 642.
 - ⁶ E. Simonotto, M. Riani, C. Seife, M. Rovers, J. Twitty, F. Moss, *Rhys. Rev. Lett*, **78** (1997) 1186.
 - ⁷ I. Hidaka, D. Nozaki, Y. Yamamoto, *Phys. Rev. Lett.*, **85**, (2000) 3740.
 - ⁸ Y. Morishita, T.J.Kobayashi, K.Aihara, *J. Theor. Biol.*, **325** (2005) 241.
 - ⁹ R. Takahashi, M. Suzuki, *Physica A*, **353** (2005) 85.
 - ¹⁰ Y. Jiang, H. Xin, *Phys. Rev. E*, **62** (2000) 1846.
 - ¹¹ A. Neiman, L. Schimansky-Geier, *Phys. Lett. A*, **197** (1995) 379.
 - ¹² J. F. Lindner, B. K. Meadows, W. L. Ditto, M. E. Inchiosa, A. R. Bulsara, *Phys. Rev. Lett.*, **75**, (1995) 3.
 - ¹³ P. Jung, P. Hänggi, *Phys. Rev. A*, **44** (1991) 8032.
 - ¹⁴ R. Kawai, A. Awazu, N. Nishimori, preparing.